Basic Visualization Experiments on Eutectic Reaction between Boron Carbide and Stainless Steel under Sodium-Cooled Fast Reactor Conditions

H. Yamano[1], T. Suzuki[1], K. Kamiyama[1], and I. Kudo[2]

[1] Japan Atomic Energy Agency (JAEA), 4002, Narita, Oarai, Ibaraki, 311-1393 Japan

[2]Advan Eng. Co., Ltd., 3399-34, Shimami, Kita-ku, Niigata, 950-3102 Japan

E-mail: yamano.hidemasa@jaea.go.jp

Abstract. This paper describes basic visualization experiments on eutectic reaction and relocation of boron carbide (B_4C) and stainless steel (SS) under a high temperature condition exceeding 1,500 °C as well as the importance of such behaviors in molten core during a core disruptive accident in a Generation-IV sodium-cooled fast reactor (750MWe class) designed in Japan. At first, a reactivity history was calculated using an exact perturbation calculation tool taking into account expected behaviors. This calculation indicated the importance of a relocation behavior of the B_4C-SS eutectic because the behavior has a large uncertainty in the reactivity history. To clarify this behavior, this study has carried out basic experiments to visualize the reaction of a B_4C block contacted with molten SS in a high temperature-heating furnace. The experiments have indicated the eutectic reaction as well as solidification of the B_4C-SS eutectic in the upper part of the solidified test section separated from the solidified SS due to the density difference.

Key Words: Sodium-Cooled Fast Reactor, Boron Carbide, Stainless Steel, Eutectic Reaction

1. Introduction

Japan Atomic Energy Agency (JAEA) has been developing a Generation IV (Gen-IV) sodium-cooled fast reactor (SFR), which is an advanced intermediate-sized (750 MWe) loop-type SFR [1], in cooperation with industrial partners. One of design concepts of Gen-IV SFRs includes in-vessel retention (IVR) that ensures long-term coolability of degraded core materials inside the reactor vessel (RV) by implementing design measures even if a core disruptive accident (CDA) occurs. To evaluate the CDA scenario, JAEA has been conducting a lot of experiments and developed assessment methodologies [2]. The effectiveness of design measures has also been evaluated to achieve IVR in the Gen-IV SFR [3]. This previous study has revealed that eutectic reactions between boron carbide (B_4C) and stainless steel (SS) as well as its relocation are one of the key issues in the CDA evaluation. Since such behaviors have never been simulated in CDA numerical analyses, it is necessary to develop a physical model and incorporate the model into the CDA analysis code.

The main objective of this study is to obtain basic experimental data to investigate the B_4C-SS eutectic reaction and relocation for the contribution to the model development mentioned above. This study is also intended to examine CDA scenarios under reactor conditions to find out the importance of the B_4C-SS reaction. The present paper describes visualization experiments under a high temperature condition exceeding 1,500 °C.

2. Importance of the B_4C-SS Eutectic Reaction Study in the CDA Evaluation

A representative CDA initiator is considered as an unprotected loss of flow (ULOF) accident in anticipated transient without scram (ATWS) events. This is because, if this accident occurs, the consequence might result in severe recriticality involving mechanical energy release in a short term although its frequency is extremely low. An advanced loop-type SFR adopts design measures that eliminate a severe recriticality [4, 5]. The CDA scenario is divided into four phases: initiating phase, early-discharge phase, relocation phase, and heat removal phase. Great experimental and numerical efforts have been made for the initiating phase and early-discharge phase, so that the assessment methodology for both phases has been advanced [3]. On the other hand, the study for the relocation phase [6, 7] still has issues to be solved, thus various investigations [8, 9] are being performed. For example, since the ingress of B_4C that absorbs neutrons into the core significantly decreases the reactivity, it is one of crucial phenomena that should be studied to reduce the potential recriticality during the relocation phase.

Although the melting temperature of B_4C is 2,500 °C, B_4C could melt below its melting temperature due to the eutectic reaction (liquefaction) if it contacts with SS [10]. The eutectic point of Fe-B alloy is about 1,200 °C [11]. Fe-B-C alloy liquefies at around the same temperature due to the eutectic reaction [12]. In the CDA scenario, degraded core could be eventually expected to melt control rod guide tubes (CRGTs) as well as cladding tube of B_4C pellets. At that time, the B_4C pellets would contact with the SS cladding tube at the temperature near the SS melting point, resulting in the eutectic reaction at the interface between the B_4C pellets and the SS cladding. The molten material formed by this reaction is then assumed to relocate widely in the core. However no quantitative assessment methodology describing such a behavior has been developed yet; it was therefore pointed out that a large uncertainty of the eutectic reaction and the relocation remains in the CDA evaluation for a large-sized SFR [3]. Hence, this eutectic reaction study is very important to reduce the uncertainty and to make the evaluation realistic and reasonable.

For an intermediate-sized loop-type SFR core [13], this paper estimates a reactivity history during the material relocation phase by using a static neutronic calculation methodology which has been applied to a large-sized loop-type SFR [3]. The early-discharge phase analysis showed that approx. 20% of molten fuel was discharged from the core and the reactivity decreased to -14$. These results are imposed to the initial conditions of the relocation phase analysis. Figure 1 illustrates a reactivity history calculated using SNPERT3D, an exact perturbation calculation code based on the neutron transport theory. Key phenomena are taken into account in estimating the reactivity history.

Since a typical SFR has two independent active reactor shutdown systems, the failure of

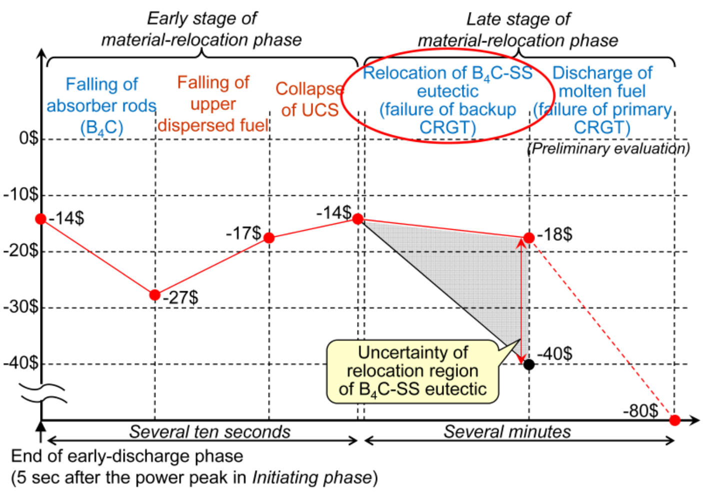

FIG. 1. Reactivity history in material relocation phase by exact perturbation calculation.

scram with the two active systems is postulated in case of the ATWS accident. To prevent this, a passive device with a Curie point magnetic alloy (called temperature sensing alloy) is incorporated into the backup shutdown system in the intermediate-sized loop-type SFR; so that the control rod could be inserted by losing the magnetic force with this temperature sensing alloy as a passive reactor shutdown system. In the ULOF event, however, this passive mechanism might be unavailable due to unforeseen reasons at a designated temperature corresponding to the Curie point of the temperature sensing alloy (e.g., 660 °C). Even in such a situation, the passive device consisting of the temperature sensing alloy and iron core would lose its magnetic force because the device at the elevation level just above the top of the fuel assembly would be exposed to a high temperature environment (exceeding 1,000 °C) formed by sodium vapor and molten material dispersed during the early-discharge phase, thereby causing the control rod (neutron absorber) insertion. In our designed SFR, the control rods that standby just above the active core can be inserted even in the end of the early-discharge phase because the plant design adopts a core restraint concept (stiff core barrel and support structures) and flexible joints for the drive line [14]. Therefore, the neutron absorber (B_4C) would be inserted into the core in the early stage of the material relocation phase, which allows decreasing the reactivity to -27$.

Contrarily, the reactivity increases to -17$ when once dispersed molten fuel falls on the upper part of the core. In addition, when upper core structures (UCSs) collapse onto the core, the reactivity increases to -14$. Hence, the reactivity change is balanced.

Although the neutron absorber in the backup control assembly is inserted into the core, its CRGT would be melted sooner or later by molten material mixture consisting of liquid SS and fuel particles in nearby fuel assemblies. The CRGT failure permits liquid SS to contact the cladding for the B_4C pellets. Eventually the SS cladding temperature would rise to its melting temperature to cause direct contact between B_4C and SS, leading to the B_4C-SS eutectic reaction. As mentioned earlier, the molten material formed by the reaction could spread in the core. If the eutectic mixes only in the neighboring six assemblies around the control rod assemblies, the reactivity reduction effect is less significant, -18$. On the contrary, if it is evenly distributed in the whole core region, the reactivity reduction effect is significant, -40$. It accounts for a large uncertainty of the behavior; and therefore it is essential to reduce the uncertainty based on the experimental data.

Since the backup CRGT is equipped with the neutron absorber rods, the volume of sodium coolant in the core region is small, that is, the heat capacity of sodium coolant in the area is small. This allows the CRGT to melt as soon as it contacts with the molten pool. On the other hand, the primary shutdown system contains a large amount of sodium in the CRGT in the core region; therefore its large heat capacity could delay the melting process. The reactivity history shown in Fig. 1 is currently at the preliminary evaluation stage. To improve this history, further efforts are being conducted to obtain precise data through additional experiments and numerical studies [15].

A reactor core of an intermediate-sized loop-type SFR [13] is designed to have six backup control assemblies that are arranged almost homogeneously in the circumferential direction in the sixth layer from the core center. We have calculated one of the assemblies' temperatures of solid particulate fuel, molten SS, CRGT wall around at the mid-plane elevation in a neighboring fuel assembly by using SIMMER code [3] as depicted in Fig. 2. This calculation was started from the initial stage of the relocation phase. The temperatures of molten SS and solid fuel are approx. 2,000 °C, whereas the CRGT wall temperature increases from about 800 °C (nearly sodium boiling temperature) to about 1,450 °C (SS melting temperature) in several hundreds of seconds. The contact between the molten SS at approx. 2,000 °C and the

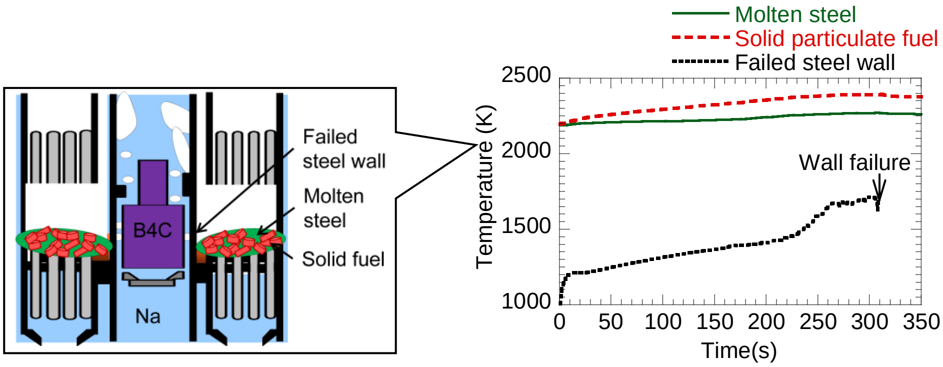

FIG. 2. Temperatures in a representative fuel assembly surrounding a control rod guide tube.

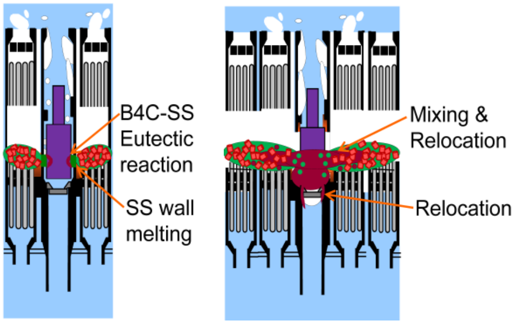

FIG.3. Important behaviors to be investigated.

B_4C cladding could be expected to increase the temperature of the cladding to its melting temperature, so that the mechanical strength of the cladding would be lost. The high temperature SS would eventually contact with the B_4C pellets. Assuming that the interface temperature reaches the SS melting temperature (approx. 1,450 °C), the eutectic temperature (approx. 1,200 °C) would be exceeded; hence the eutectic reaction would occur. Moreover, the acceleration of its reaction could be expected by further contact between B_4C and SS with time because the liquid SS of the CRGT and cladding would be mixed near the control assembly.

Figure 3 shows important behaviors to be investigated including the B_4C-SS reaction and relocation of the eutectic. These behaviors need to be simulated in experiments.

3. Basic Visualization Experiment on B_4C-SS Eutectic Reaction

3.1. Experiment Apparatus and Methods

An experimental apparatus of a graphite heater furnace is shown in Fig. 4 [16]. In the furnace filled with argon gas, a test section container (150 x 150 x 50 mm long and 5 mm thick) made of alumina was placed in the middle of two heaters (260 mm in distance between the heaters) on a tray. On the test section, an alumina crucible filled with SS was set to pour liquid SS into the test section with a gravity fall mechanism. The furnace has a window to visualize the reaction using a video camera. A W-Re thermocouple was used to measure each temperature of the SS in the crucible and the test section containing B_4C. The additional thermocouple was employed for the measurement of the atmospheric temperature in the furnace. A radiation pyrometer measured the graphite heater temperature.

A cube shaped B_4C block (approx. 50 x 30 x 25 mm) with 95% theoretical density was used to make the observation of the contact interface easier. The B_4C block was covered laterally with alumina blocks, which were rolled by tantalum wire, to fix. An alumina crucible (110 mm in diameter at the upper level, 100 mm in height) was filled with 2.1 kg of SS316

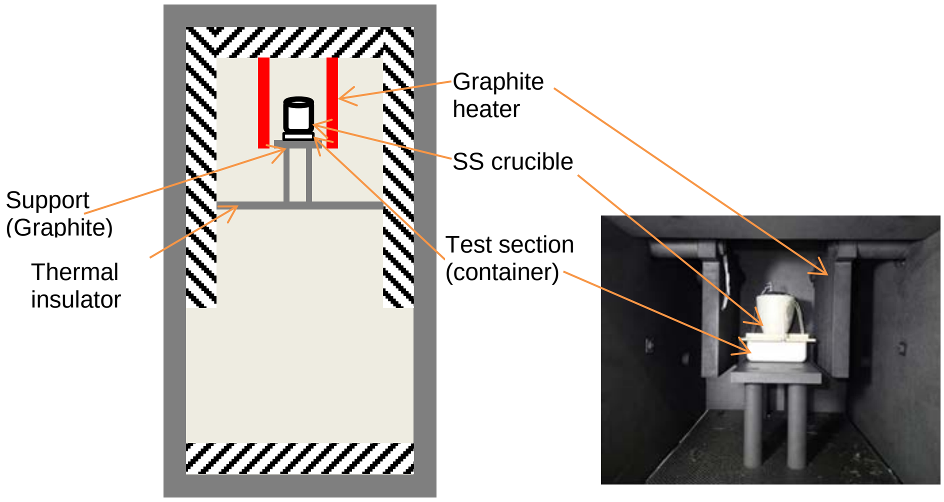

(a) Heating furnace *(b) Test section*

FIG. 4. Experimental apparatus.

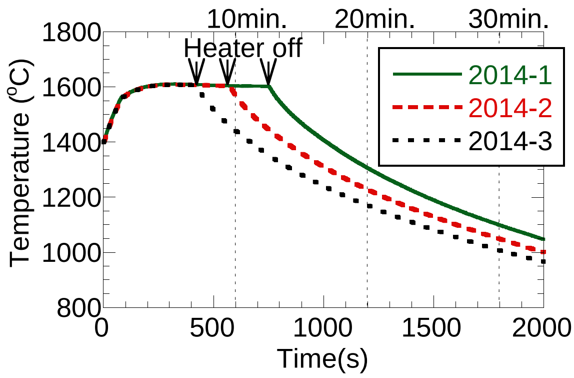

FIG. 5. Heater temperatures.

corresponding to the reactor material. This crucible has a 15 mm hole on its bottom surface to fall molten SS on the test section when SS melts.

Three experimental cases with different heating patterns were performed as shown in Fig. 5. The starting time of temperature increase at 1,400 °C is 0 in this figure. The test section was gradually heated from room temperature for several hours after the atmosphere in the furnace was replaced from air to argon gas. At 1,000 °C, we waited until the temperature of the entire interior became equilibrium, and then gradually heated it again. The same procedure was repeated at 1,400 °C, and the transient experiment was started by a rapid heating from 1,400 °C to a prescribed heater temperature of 1,600 °C which is close to the maximum power of the furnace. To examine effect of B_4C-SS contact duration on the relocation behavior of the eutectic. Therefore, the experimental parameter is a power-off time of the heating (heater temperature retention time) at 1,600 °C; approx. 6 min., 3 min. and 0 min. after the B_4C-SS contact were used for Case 2014-1, 2014-2 and 2014-3 (named in this paper), respectively.

Before these experiments, we carried out a preliminary experiment (named Case 2014-0) by heating it for 43 minutes. In spite of no temperature measurement, the post-test observation of the solidified eutectic is useful information to discuss in this paper.

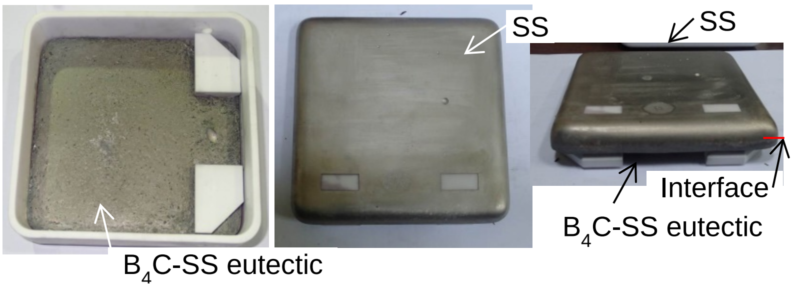

FIG. 6. Post-test observation in Case 2014-0.

3.2. Experimental Results and Observations

3.2.1. Case 2014-0

The event sequences are as follows. Note that several seconds are included as a measurement error since these were determined based only on the images obtained through the visualization.

5 min. 25 s: SS melting start
14 min. 09 s: SS falling start
14 min. 41 s: B_4C contact with SS
17 min.25 s: SS falling stop
43 min. 15 s: B_4C separation
48 min. 21 s: Heater power-off

Figure 6 shows the upper and bottom surfaces of the test section after the experiment with the side view. The B_4C block melted completely on the upper surface. Looking at the side view, the interface between the B_4C-SS eutectic on the upper surface and solidified SS on the bottom can be clearly observed. This result suggests that both the materials are separated due to their density difference. The B_4C block remained for a long time in spite of a high temperature condition which could be higher than the eutectic temperature. This result has given the evidence that the B_4C can be melted if the hot condition is continued for a long time.

3.2.2. Case 2014-1

Figure 7 shows temperatures of the heater, the furnace interior, the test section, and the SS crucible measured by the thermocouple in Case 2014-1. Figure 8 shows visualization test results taken by the video camera. First, the SS melted in the crucible, then dropped on the test section and contacted with the B_4C block. The B_4C-SS eutectic reaction is observed. Finally, we observed the separation of the remaining part of the B_4C block from the original location and the B_4C floating behavior on the liquid SS pool. The event sequences are as follows. In this case, the heater was turned off in about six minutes after the B_4C-SS contact.

1 min. 32 s: SS melting start
7 min. 07 s: SS falling start
7 min. 32 s: B_4C contact with SS
10 min.42 s: SS falling stop
13 min. : Eutectic reaction stop
13 min. 19 s: Heater power-off
14 min. 07 s: B_4C separation

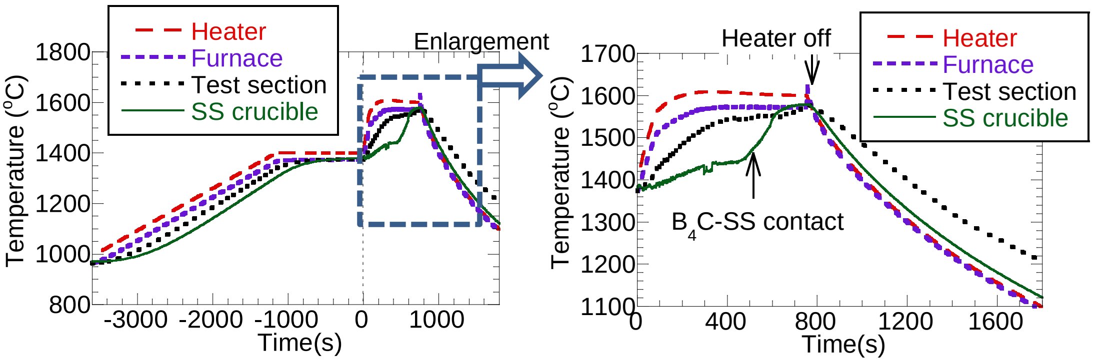

FIG. 7. Temperatures in Case 2014-1.

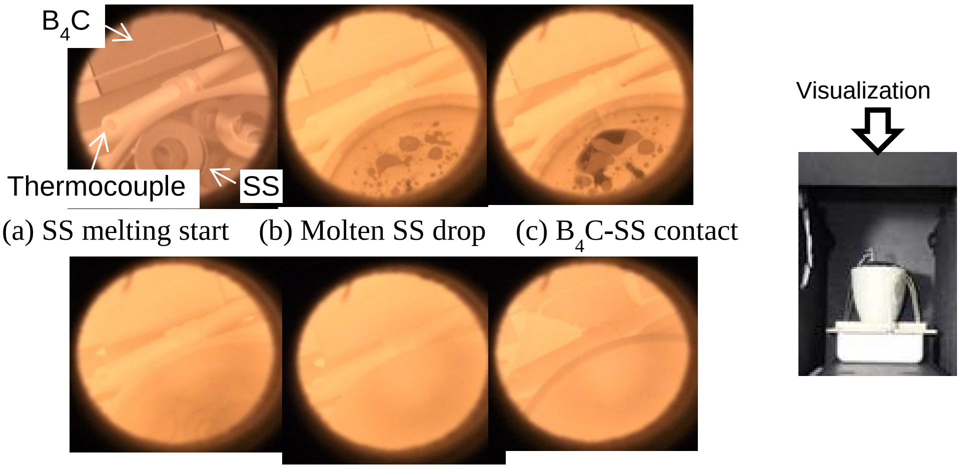

FIG. 8. Visualization of B_4C-SS eutectic reaction in Test 2014-1.

Judging from the visualization images and thermocouple data, SS in the crucible started melting at 1,380 °C and started falling at 1,440 °C, which could be distributed inside the crucible. Figure 9 shows the temperatures of the test section in Case 2014-1, 2014-2 and 2014-3. In all the cases, B_4C contacted with SS when the temperature reached at 1,544 °C, which is a high enough temperature to cause the eutectic reaction. At around 1,550 °C, SS stopped falling. Gradual temperature increase was seen until the heaters were turned off.

Figure 10 shows the upper and bottom surfaces of the test section after the experiment. After the tantalum wire was damaged, the B_4C block separated with floating and then solidified on the surface of the eutectic melt pool. The lighter density of B_4C (approx. 2,500 kg/m^3) than

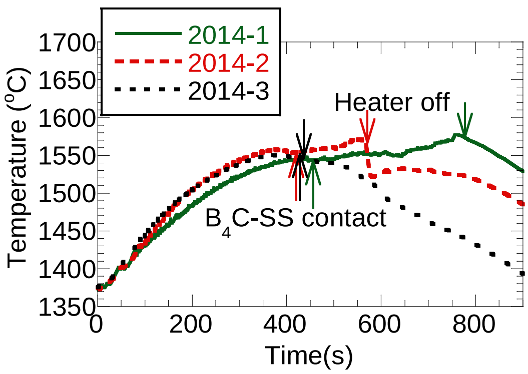

FIG. 9. Temperatures at B_4C block surface. (arrow colors correspond to test cases).

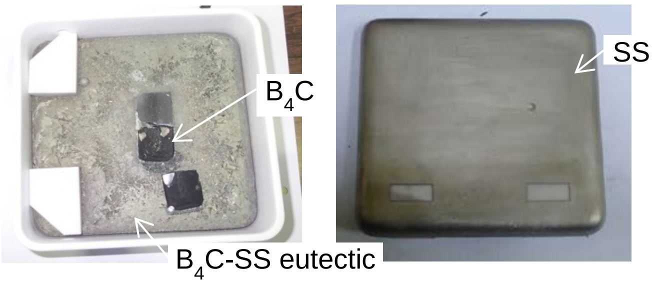

FIG. 10. Post-test observation in Case 2014-1.

SS and the B_4C-SS eutectic can account for the separation. As demonstrated in the past [10], it can be said that dendrite structure appeared on the upper surface is the B_4C-SS eutectic. On the bottom surface, contrarily, solidified SS is seen. This observation revealed that the density difference between the B_4C-SS eutectic and the SS separated from each other.

3.2.3. Case 2014-2

The following event sequences were observed from the video images. In this case, the heater was turned off in about three minutes after the B_4C-SS contact.

1 min. 24 s: SS melting start
6 min. 11 s: SS falling start
7 min. 0 s: B_4C contact with SS
9 min. 33 s: SS falling stop
9 min. 37 s: Heater power-off
15 min. : Eutectic reaction stop

Figure 11 shows the temperatures observed in Case 2014-2, which are very similar to the results of 2014-1. When the eutectic reaction stopped, the test section was at 1,485 °C. The reaction should have had continued even under this temperature condition; however the

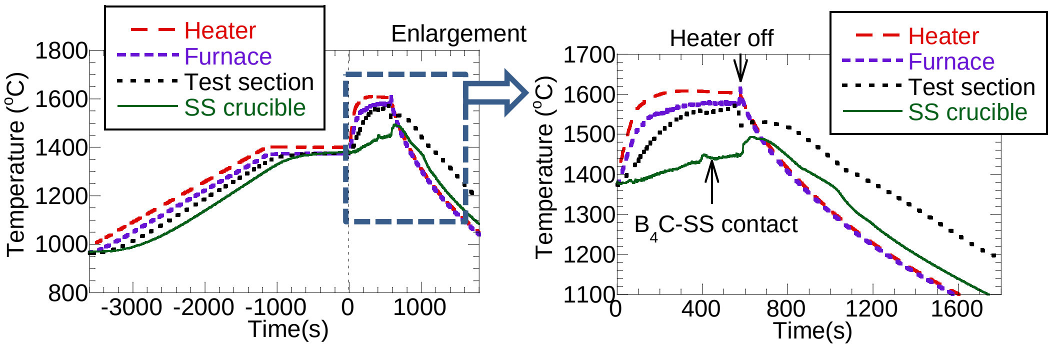

FIG. 11. Temperatures in Case 2014-2.

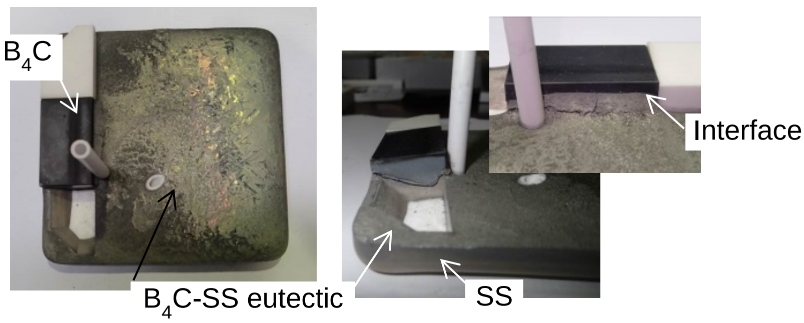

FIG. 12. Post-test observation in Case 2014-2.

eutectic reaction stopped. This is because another eutectic material in slightly different color from the one appeared on the upper surface laid between the B_4C block and the SS pool impeded their direct contact for the reaction.

Figure 12 shows the upper and the side surface of the test section after the experiment, as well as the reaction interface of the B_4C block. Since the B_4C block was firmly fixed, we could obtain the reaction interface without the block separation. At the interface between B_4C block and the eutectic, a certain material with difference color can be seen, which is similar observation in the past study [17]. The image indicates that the whole bottom part of the B_4C block submerged in the molten SS had the reaction, and then the B_4C-SS eutectic melt has spread over the SS region around 150 mm, which is a width of the container including the test section. It took about 18 minutes before the test section temperature reached 1,400 °C, nearly corresponding to the SS solidus temperature.

3.2.4. Case 2014-3

In this case, the heater was turned off as soon as the B_4C-SS eutectic contacted. From the video images, the event sequences were seen as follows.

1 min. 40 s: SS melting start
6 min. 28 s: SS falling start
7 min. 12 s: B_4C contact with SS, heater power-off
11 min. 8 s: SS falling stop
21 min. : Eutectic reaction stop

Figure 13 shows the temperatures at each behavior observed in Case 2014-3, which are very similar to the results of Case 2014-1 and 2014-2.

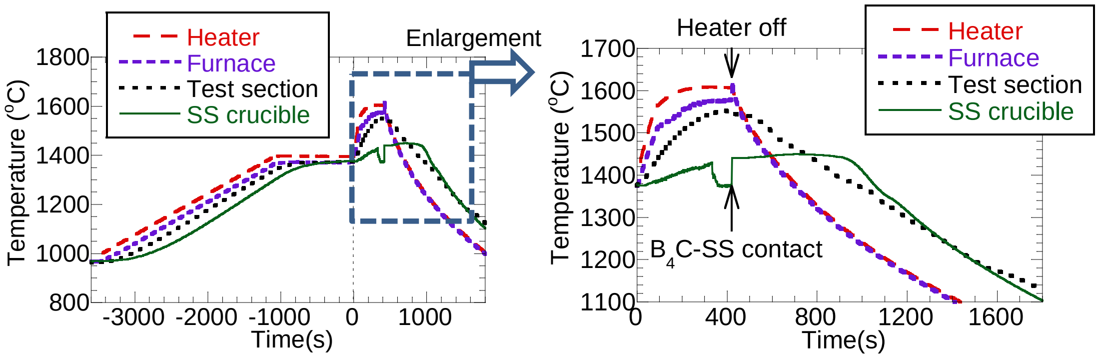

FIG. 13. Temperatures in Case 2014-3.

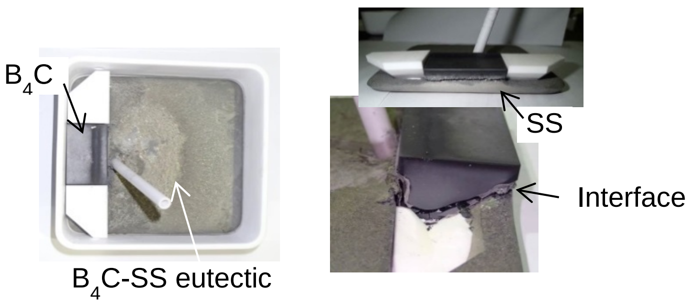

FIG. 14. Post-test observation in Case 2014-3.

Post-test photos of the test section in Case 2014-3 are shown in Fig. 14. Compared to Case 2014-2, the bottom part of B_4C block remained more and the amount of eutectic on the contact interface was less. It took about ten minutes before the temperature of the test section reached 1,400 °C. Molten SS kept falling when it started solidifying, thus the eutectic reaction continued comparably longer; because the contact interface remained longer, the reaction completed later than Case 2014-2. When it completed, the test section was at 1,276 °C, which is consistent with higher than the eutectic temperature (1,200 °C) obtained in the past study. The B_4C-SS eutectic moved to the center of the container about 60 mm before SS solidifies.

4. Conclusion

This study has shown the importance of B_4C-SS eutectic reaction and the relocation behaviors under the high temperature condition by conducting evaluations on reactivity change in the relocation phase and on temperatures of degraded core materials around the backup control rods during a postulated CDA in the SFR. This basic experiment on B_4C-SS reaction has successfully visualized the eutectic reaction between B_4C and SS, as well as relocation and separation between B_4C, the eutectic, and SS due to their density difference.

Acknowledgments

This document includes the result of "Technology development of fast breeder reactors, etc.” entrusted to Japan Atomic Energy Agency (JAEA) by the Ministry of Economy, Trade and Industry (METI).

References

[1] KAMIDE. H., et al., “JSFR Design Progress Related to Development of Safety Design Criteria for Generation-IV Sodium-Cooled Fast Reactors (1) Overview,” Proc. 23rd Int. Conf. of Nucl. Eng., JSME, Makuhari, Japan (May 17-21, 2015) ICONE23-1666.

[2] TOBITA, Y., et al., “Development of the Evaluation Methodology for the Material Relocation Behavior in the Core Disruptive Accident of Sodium-Cooled Fast Reactors,” J. Nucl. Sci. Tech., **53**(5) (2016) 698-706.

[3] SUZUKI, T., et al., “A Scenario of Core Disruptive Accident for Japan Sodium-Cooled Fast Reactor to Achieve In-Vessel Retention,” J. Nucl. Sci. Tech., **51**(4) (2014) 493-513.

[4] ENDO, H., et al., “Elimination of Recriticality Potential for the Self-Consistent Nuclear Energy System,” Prog. Nucl. Ener., **40**(3-4) (2002) 577-586.

[5] TOBITA, Y., et al., “Analytical Study on Elimination of Severe Recriticalities in Large Scale LMFBRs with Enhancement of Fuel Discharge,” Nucl. Eng. Des., **238**(1) (2008) 57-65.

[6] KOYAMA, K., et al., “Development of Level 2 PSA Methodology for Sodium-Cooled Fast Reactors (4) Development of Technical Basis in the Material-Relocation and Decay-Heat Removal Phases of Unprotected Events,” Proc. 8th Int. Top. Mtg. on Nucl. Thermal-Hydraulics, Operation and Safety (NUTHOS-8), CNS, Shanghai, China (2010) N8P0102.

[7] SUZUKI, T., et al., “Development of Level 2 PSA M1ethodology for Sodium-Cooled Fast Reactors - Overview of Evaluation Technology Development -,” OECD, NEA/CSNI/R(2012)2 (2012) 381-391.

[8] KAMIYAMA, K., et al., “An Experimental Study on Heat Transfer from a Mixture of Solid-Fuel and Liquid-Steel during Core Disruptive Accidents in Sodium-Cooled Fast Reactors,” Proc. 10th Int. Top. Mtg. on Nucl. Thermal-Hydraulics, Operation and Safety (NUTHOS-10), AESJ, Ginowan, Japan (2014) No.1050.

[9] MATSUBA, K., et al., “Experimental Discussion on Fragmentation Mechanism of Molten Oxide Discharge into a Sodium Pool,” Proc. Int. 23rd Conf. of Nucl. Eng., JSME, Makuhari, Japan (2015) ICONE23-1603.

[10] NAGASE, F., et al., “Chemical Interactions between B_4C and Stainless Steel at High Temperatures,mpJ. Nucl. Mat., 245 (1997) 52-59.

[11] MASSALSKI, T.B., Binary Alloy Phase Diagram (1990) 482.

[12] SUDO, A., et al., “Fundamental Experiments on Phase Stabilities of Fe-B-C Ternary Systems,” J. Nucl. Sci. Tech., **52** (2015) 1308-1312.

[13] OGURA, M., et al., “Conceptual Design Study on Core toward the Demonstration Reactor of JSFR (2) Core Design,” Trans. AESJ 2010 fall Mtg. (2010) P31.

[14] YAMANO, H., et al., “Safety Design and Evaluation in a Large-Scale Japan Sodium-Cooled Fast Reactor,” Science and Technology of Nuclear Installations, Article ID 614973 (2012) doi:10.1155/2012/614973.

[15] KAMIYAMA, K., et al., “Development of an Evaluation Methodology for Fuel Discharge in Core Disruptive Accidents of Sodium-Cooled Fast Reactors,” J. Ener. Pow. Eng., **8** (2014) 785-793.

[16] KURATA, M, et al., “Upgrade of Analytical Methodology of Fuel Failure and Melting Phase during Severe Accidents – Project Overview and Current Status –,” Trans. AESJ 2014 fall Mtg. (2014) TN03.

[17] SHIBATA, H., et al., “Chemical Interaction between Granular B_4C and 304L-Type Stainless Steel Materials Used in BWRs in Japan,” J. Nucl. Sci. Tech., **52**(10), (2015) 1313-1317.